

Asymptotic D -state to S -state ratio of the deuteron

N. L. Rodning* and L. D. Knutson

University of Wisconsin, Madison, Wisconsin 53706

(Received 16 August 1989)

The asymptotic D -state to S -state ratio of the deuteron (η) is deduced from new measurements of tensor analyzing powers in sub-Coulomb (d,p) reactions. The complete set of analyzing power measurements is presented. Ten statistically independent values are obtained for η from measurements of two analyzing powers using multiple targets, final states, and beam energies. These values are consistent to within their statistical uncertainties. A weighted average of the individual values gives the result $\eta=0.0256\pm 0.0004$, where the quoted uncertainty includes systematic and statistical contributions. This result is compared with previous measurements and with the predictions obtained from a variety of theories.

I. INTRODUCTION

The deuteron D -state has been a subject of interest in nuclear physics for decades. The D -state admixture accounts for the nonzero deuteron quadrupole moment, and indicates that the nucleon-nucleon interaction contains noncentral terms. Traditionally, interest in the deuteron D state was centered on the D -state probability, P_d . However, it has been shown¹ that when one includes mesonic degrees of freedom the D -state probability is not well defined (i.e., the value of P_d depends on the representation chosen to describe the deuteron bound state). As a result, recent interest in the deuteron D state has focused on the asymptotic D -state to S -state ratio (η), now widely considered the fundamental D -state observable.

In an earlier letter² we described a series of measurements from which we extracted a value for η . For reasons that will be described below, we believe this to be the most reliable determination available to date. Our value of η was obtained by comparing measurements of tensor analyzing powers in (d,p) reactions on heavy nuclei at incident energies well below the Coulomb barrier to calculations of the analyzing powers made with the distorted wave Born approximation (DWBA). The purpose of the present paper is to provide further experimental details, to describe the analysis in more detail, and to comment on the status of empirical and theoretical knowledge of the asymptotic D -state to S -state ratio of the deuteron.

In the following section we will summarize the previous measurements of η and comment on the reliability of the techniques employed. The experimental details will be presented in Sec. III. This section also contains a description of the polarimeter calibration experiment which was used to determine the normalization of the analyzing power measurements. A description of the DWBA analysis is presented in Sec. IV, along with a discussion of the uncertainties in the calculations and a description of the method used to extract a value for η from the measurements. Our final result for η is presented in Sec. V, and the comparison with previous empirical and theoretical values is discussed in Sec. VI.

II. EMPIRICAL DETERMINATIONS OF η

A. Previous measurements

In the past, two techniques have been employed to determine η . One method involves the pole extrapolation of tensor analyzing power measurements for $d-p$ elastic scattering and the ${}^2\text{H}(d,p){}^3\text{H}$ reaction, while the other involves the analysis of tensor analyzing power data for sub-Coulomb (d,p) reactions. Several empirical and theoretical values³⁻¹⁴ for η are listed in Table I.

The amplitudes for $d-p$ elastic scattering and for the ${}^2\text{H}(d,p){}^3\text{H}$ reaction contain a neutron exchange term which becomes infinite (i.e., has a pole) at an angle which is related to the bombarding energy and the deuteron binding energy. Since the pole residues depend on the asymptotic normalization constants of the deuteron wave function, the scattering observables at the pole have a simple relationship to η .¹² For physical values of the incident deuteron energy, the singularity occurs at an unphysical angle. Because the scattering observables cannot be directly measured at this angle, the conventional approach has been to determine η by extrapolation of measurements obtained within the physical region.

A number of values for η which appear in the literature have been obtained using the pole-extrapolation technique, applied most often to $d-p$ elastic scattering.^{9-12,14} Unfortunately, the uncertainty quoted for these values omits possible errors in the extrapolation. Systematic uncertainties in the extrapolation arise because the extrapolation function may differ in some systematic way from the true physical function which is being extrapolated. Traditionally, a finite series has been used as the extrapolating function. For the case of pole extrapolations in $d-p$ elastic scattering, it has been shown that truncation of the series expansion may lead to errors in η of as much as 10-20% or more.¹⁴⁻¹⁷ A careful study of extrapolation errors in the ${}^2\text{H}(d,p){}^3\text{H}$ reaction has not yet been undertaken, but we have no reason to believe that the systematic uncertainties should be smaller.

Data obtained in $d-p$ elastic scattering have also been

TABLE I. Values of η as calculated using various deuteron models. Also listed are several experimental results for η . The quoted uncertainty for each measurement, and for some of the calculations, is shown in parentheses.

Method	η	Reference
Theoretical results		
RSC potential	0.0262	3
RHC potential	0.0259	3
Paris potential	0.0261	4
OPE dominance	0.0259(3) ^a	5
Schwartz inequality	0.0268(7)	6
Phase shift analysis of <i>n-p</i> elastic scattering	0.027 12(22)	7
Experimental results		
Sub-Coulomb (<i>d,p</i>)	0.0271(8)	8
Pole extrapolation:		
<i>d-p</i> elastic scattering	0.0270(6) ^b	9
<i>d-p</i> elastic scattering	0.0259(7) ^{b,c}	10
<i>d-p</i> elastic scattering	0.0263(13) ^{b,c}	11
<i>d-p</i> elastic scattering	0.027(5) ^{b,c}	12
² H(<i>d,p</i>) ³ H	0.0272(4) ^b	13
Fitting data for <i>d-p</i> elastic scattering	0.0264(14)	14

^a Obtained from Eq. (17) of Ref. 5, with $f^2=0.0776(9)$, and with $\Lambda \rightarrow \infty$.

^b Quoted uncertainty omits possible errors in the extrapolation procedure.

^c Result obtained neglects a correction for the Coulomb amplitude (Ref. 17).

analyzed by Londergan *et al.*¹⁴ using a technique which does not require extrapolation beyond the physical region. Since the scattering amplitude within the physical region contains contributions from several other processes, in addition to the neutron exchange process, these authors have written the scattering amplitude as a sum of the terms which are expected to dominate. Several free parameters in the expression (including η) are then allowed to vary to obtain an optimum fit to the data. The result obtained for η in this way has an accuracy of about 5%.

A value for η has also been extracted from previous measurements of tensor analyzing powers in sub-Coulomb (*d,p*) reactions.^{8,18} This technique relies on the fact that—to a good approximation—tensor analyzing powers in these reactions depend only on η .¹⁹ The best value previously obtained for η by this method (see Table I) was extracted from measurements of tensor analyzing powers in the ²⁰⁸Pb(*d,p*)²⁰⁹Pb reaction at 7.0, 8.0, and 9.0 MeV. In this experiment, systematic uncertainties arise from the fact that the optical potentials used in the calculations are not known precisely. The result quoted in Table I includes this systematic uncertainty as well as the statistical uncertainty in η .

Of the two methods, the sub-Coulomb (*d,p*) technique has the advantage that the analysis relies on a model (DWBA) in which the approximations being made are well understood. This makes it possible to readily examine and quantify possible sources of systematic error. On the other hand, we know of no procedure that leads to a realistic quantitative estimate of the truncation errors which are inherent in conventional pole-extrapolation analyses.

B. Present measurements

We have extracted a value for η from new measurements of tensor analyzing powers in sub-Coulomb (*d,p*) reactions. We have made considerable effort to improve the reliability and precision of this result over the value previously obtained utilizing this technique.^{8,18}

To decrease the influence of nuclear interactions on the reaction process, we have made measurements at lower incident energies. We have also obtained measurements for two target nuclei, which gives us a consistency check on the accuracy of the DWBA analysis.

Another improvement over previous work results from our ability to switch rapidly between positive and negative polarization states. Because the determination of the analyzing powers requires comparison of counting rates obtained with two or more beam polarization states, it is important that changes in count rate which are not related to the change in beam polarization are minimized. By employing fast switching of the beam polarization we were able to reduce the influence of slow changes in the counting rate caused by variations in factors such as target thickness, beam energy and position, and detector gain which could in principle have influenced previous measurements.

Finally, we have made an independent absolute calibration of the deuteron tensor polarimeter. This calibration was obtained using the ¹⁶O(*d,α*)¹⁴N reaction. The calibration also benefits from fast switching of the beam polarization and from care taken in monitoring and eliminating contaminant states from the reaction spectra.

With these improvements in the reliability of the sub-Coulomb technique for extracting η , we believe that our

value for η is the most reliable empirical value available to date.

III. DESCRIPTION OF THE EXPERIMENT

A. The (d,p) measurements

We have measured the analyzing power (Ref. 20) T_{20} of the $^{208}\text{Pb}(d,p)^{209}\text{Pb}$ reaction at 6.0 and 7.0 MeV, the analyzing power T_{21} of the same reaction at 7.0 MeV, and the analyzing power T_{20} of the $^{136}\text{Xe}(d,p)^{137}\text{Xe}$ reaction at 4.5 and 5.5 MeV. In each case, we have obtained measurements for two final states so that altogether we have a total of ten angular distributions. The measurements were made at the University of Wisconsin electrostatic accelerator laboratory using polarized deuterons produced with a crossed-beam ion source.²¹

For all measurements the sign of the beam polarization was cycled between positive, negative, and unpolarized states at intervals of less than 1 s. For the T_{20} measurements, the spin-alignment axis of the beam was along the beam momentum direction, so that the t_{20} component of the beam was maximized while other components of the beam polarization were nearly zero. The polarization of the beam was measured with a polarimeter located downstream of the principle reaction chamber. For T_{20} measurements, the analyzing power in the (d,p) reactions was determined by using the expression

$$T_{20} = \frac{1-R}{Rt_{20}^- - t_{20}^+}, \quad (1)$$

where

$$R = \frac{F^+}{F^-}. \quad (2)$$

Here F^+ and F^- represent the ratio of the number of counts to the integrated charge obtained with beam polarizations t_{20}^+ and t_{20}^- , respectively.

The data obtained from detectors placed left and right of the beam were used to determine two values for T_{20} which were subsequently used in forming a weighted average. Any contributions from small nonzero t_{21} and it_{11} polarization components in the beam cancel in taking this average. In our experiment t_{22} is very small compared to t_{20} . This coupled with the fact that T_{22} is small for the reactions being studied means that the resulting fractional error in T_{20} values is on the order of 0.1%.

For the T_{21} measurements, the spin-alignment axis of the beam was oriented at 45° with respect to the beam momentum direction. This orientation was chosen to maximize the t_{21} component of the polarization. For these measurements, we use the expression

$$T_{21} = \frac{1}{4t_{21}^\pm} \left[\frac{F_L^\pm}{F_L^o} - \frac{F_R^\pm}{F_R^o} \right], \quad (3)$$

where the F 's have the same definition as before. In this case the subscripts L and R refer to detectors located to the left and right of the beam, while the superscript "o" refers to the state for which the beam is unpolarized.

Data obtained with an unpolarized direct extraction source were used to verify that the residual polarization of the crossed beam source had negligible impact on the measured analyzing powers.

From Eq. (3) we obtain two values of T_{21} , one for each of the two polarization states. These results were averaged together. The nonzero t_{20} and t_{22} components of the beam polarization do not contribute to T_{21} as calculated by Eq. (3). A nonzero it_{11} component could contribute in principle, but the largest possible contribution is negligible.

For the ^{208}Pb measurements, a special chamber was constructed to minimize the contamination of the target by oxygen, nitrogen, and carbon. The design allowed us to produce the targets within the scattering chamber by evaporating isotopically enriched ^{208}Pb onto a carbon backing. By rotating an axle, these targets could be moved into the path of the beam without exposure to the atmosphere. A series of clean vacuum pumps produced an operating pressure of about 10^{-8} Torr in the scattering chamber during target production as well as during data acquisition.

The target used in these measurements consisted of about $500 \mu\text{g}/\text{cm}^2$ of ^{208}Pb on a $3\text{-}\mu\text{g}/\text{cm}^2$ carbon backing. Protons were detected in each of four solid-state detector telescopes, arranged symmetrically left and right of the beam. Each telescope consisted of a thin solid-state ΔE detector followed by an E detector thick enough to stop all reaction products. The thicknesses of the ΔE detectors were chosen so that the elastically scattered deuterons would stop, or nearly stop, in the ΔE detector, whereas protons from the reactions of interest would pass through and deposit a substantial amount of energy in the E detector. This system makes it possible to eliminate deuterons and heavier particles from the spectrum by placing a lower-level discriminator on the E -detector signal and using this to gate the pulses sent to the analog-to-digital converter (ADC's). One advantage of this simple particle-identification scheme is that the electronic dead times can be kept small in spite of the high elastic scattering count rate.

The detectors were located 11.4 cm from the target. Circular slits made of 0.1-mm Ta were used to define detector solid angles of 7 msr. The detectors were also equipped with a slit assembly that restricted the field of view to a small region around the target. The beam was defined by 1.0-mm (horizontal) by 1.5-mm (vertical) slits located 14.9 cm upstream of the target. A feedback system was used to center the beam on these slits. To minimize scattering from the edges of the slits, these slits were also made of thin (0.1 mm) Ta foil. A circular anti-scattering slit 7.6 cm downstream of the beam defining slits was used to prevent particles which scattered from the edges of the beam defining slit from hitting the target frame.

A sample spectrum from the $^{208}\text{Pb}(d,p)^{209}\text{Pb}$ reaction is shown in Fig. 1(a). We have chosen to show this spectrum since it illustrates some of the difficulties involved in extracting the reaction peak sums. This spectrum was obtained with an incident deuteron energy of 6.0 MeV and a detector angle of 130° . Notice that in addition to

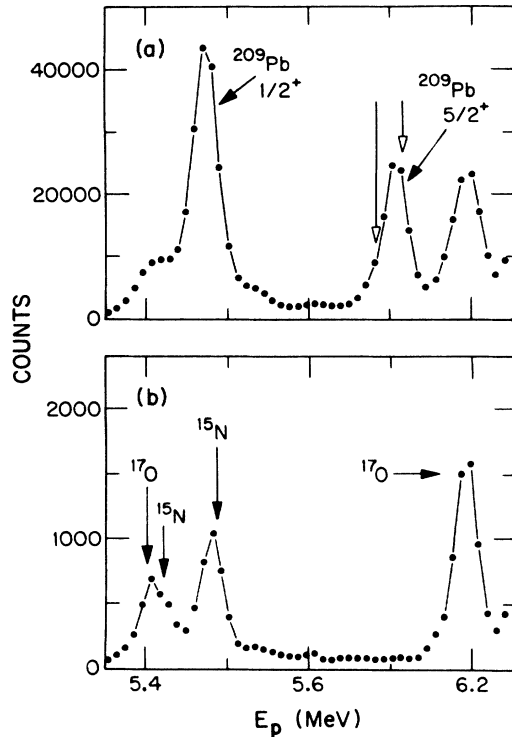


FIG. 1. Sample pulse-height spectra for an incident deuteron energy of 6.0 MeV and a detector angle of 130° . (a) shows the spectrum obtained with a ^{208}Pb target, and (b) shows the spectrum obtained with a carbon target. The vertical arrows in (a) show the summation limits used in obtaining the peak sum for the $\frac{5}{2}^+$ final state.

proton groups from reactions on ^{208}Pb , protons from reactions on ^{16}O and ^{14}N are also visible. Because these contaminant nuclei are much lighter than ^{208}Pb , the contaminant peaks move through the ^{208}Pb peaks as the detector angle is changed. For angles at which the contaminant contribution to the peak sum was greater than 10%, the data were rejected. This resulted in gaps in the angular distribution. For cases in which the contaminant contribution was small we made a correction by measuring spectra for targets with no Pb.

We found that a blank carbon target backing contained sufficient oxygen and nitrogen that it could be used for this purpose. A carbon spectrum obtained at $E = 6.0$ MeV, $\theta = 130^\circ$, is shown in Fig. 1(b). Note that the region under the peak corresponding to the $\frac{5}{2}^+$ final state in ^{209}Pb ($E_x = 1.57$ MeV) is essentially free of contaminant counts. By choosing narrow summation limits for this peak (shown by the open-headed arrows), we were able to assure that the $^{16}\text{O}(d,p)^{17}\text{O}$ reaction did not contribute to the peak sum. On the other hand, we found that about 23% of the counts in the proton group associated with the $\frac{1}{2}^+$ state ($E_x = 2.03$ MeV) actually are products of reactions on contaminants. Because a large correction is required, the $\frac{1}{2}^+$ data at this angle were discarded.

At 7 MeV the contaminant peaks are less of a problem, since the $^{208}\text{Pb}(d,p)^{209}\text{Pb}$ cross sections are larger by a factor of 7 than at 6 MeV. Nevertheless, there were still

some angles at which it was necessary to reject the data for one of the two final states.

The random background under the peaks was typically 2% of the ^{208}Pb peak sum at 7.0 MeV, and 10% at 6.0 MeV. This background was subtracted away by assuming that the background was flat, and that channels near the peak were representative of the region beneath the peak. Several regions adjacent to the peak of interest were used to characterize the background correction. The standard deviation in results obtained using different regions was taken as a measure of the systematic error in the background subtraction. The net uncertainty in the background subtraction was found by adding this systematic error in quadrature with the statistical error in the background correction.

In general we used narrow windows for obtaining the peak sums, in order to minimize the harmful effect of background and contaminants. Since we use rapid spin switching, the peak shape should be identical for the two spin states and as a result one can use any portion of the peak to determine the analyzing power. In order to check the reliability of the contaminant and background corrections we carried out a "channel-by-channel" analysis of the data.²² In this type of analysis one makes use of the fact that if all the counts in the peak region

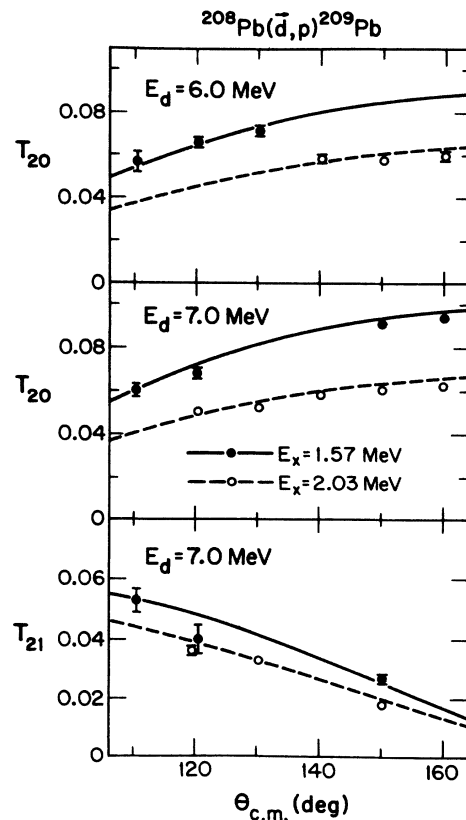


FIG. 2. Comparison of DWBA calculations with measurements of the tensor analyzing powers in (d,p) reactions on ^{208}Pb . The error bars on the measured points include the statistical uncertainty and the uncertainty in the background corrections; the uncertainty in the normalization is not included. The curves have not been adjusted to fit the data.

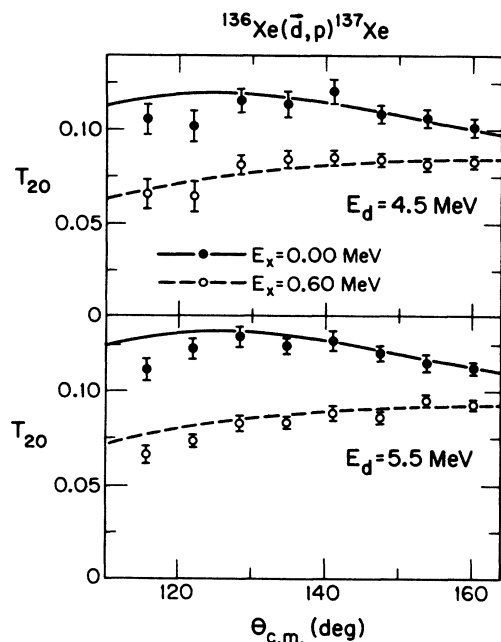


FIG. 3. Comparison of DWBA calculations with measurements of the tensor analyzing powers in (d,p) reactions on ^{136}Xe . The comments for Fig. 2 apply.

arise from a single reaction, then the analyzing power for individual channels in the peak region should be the same to within the statistical errors.

The ^{136}Xe data were obtained with a thin walled gas cell operated at a pressure of 50 Torr. The entrance and exit foils of the cell consisted of 250- μm -thick Havar. In this case the determination of the peak sums was much more straightforward. Only one contaminant peak [$^{12}\text{C}(d,p)^{13}\text{C}$] was found in the interesting portion of the spectra, so that a small (approximately 7%) correction to the peak sums was required for data obtained at some angles at an incident energy of 4.5 MeV. In this case the contaminant spectra were obtained by filling the gas cell with methane.

The analyzing power measurements are shown in Figs. 2 and 3. In each case, the curves are the result of finite range DWBA (Ref. 23) calculations which are described further in Sec. IV.

B. Polarimeter calibration

The overall normalization of the measured analyzing powers is fixed by making an absolute calibration of the polarimeter.²⁴ In order to reduce the normalization uncertainty to the 1% level, an auxiliary experiment was undertaken to improve the accuracy of the absolute calibration for T_{20} measurements at the specific energies used in the (d,p) experiments. The calibration was obtained by using the $^{16}\text{O}(d,\alpha)^{14}\text{N}$ reaction. For this reaction, conservation of parity constrains the analyzing powers to be known constants²⁵ independent of energy and angle. Consequently, this reaction can be used as a primary polarization standard, and serve as the basis for

establishing secondary standards.

For the purpose of the T_{20} measurements, the calibration consists of measuring the T_{20} analyzing power for the $^3\text{He}(d,p)^4\text{He}$ reaction at zero degrees in the polarimeter. The calibration experiment (including results for the T_{22} polarimeter analyzing powers) is described in greater detail in Ref. 26. As in the (d,p) experiment, fast switching of the beam polarization was used to eliminate systematic errors resulting from gain shifts, changes in the beam tuning, and variations in the target density, etc.

For the calibration experiment, the scattering chamber was filled with natural oxygen at pressures of between 22 and 37 Torr. The beam entered the chamber through a 0.5- μm -thick Ni foil and, after passing through the oxygen gas and a 2.5- μm -thick Havar exit foil, entered the polarimeter. Because the reaction of interest does not conserve isospin, the cross section is small, and the primary difficulty in the calibration is to obtain clear spectra with little background under the $^{16}\text{O}(d,\alpha)^{14}\text{N}$ peak. By adjusting the oxygen pressure in the chamber, we were able to fix the energy loss in the gas so as to exploit resonances²⁷ in the $^{16}\text{O}(d,\alpha)^{14}\text{N}$ reaction while at the same time arranging that the deuteron energy in the polarimeter was appropriate for matching the conditions of the (d,p) experiments. Alpha particles from the $^{16}\text{O}(d,\alpha)^{14}\text{N}$ reaction were detected in four detectors located symmetrically left, right, above, and below the beam at a laboratory angle of 20° . For data obtained with unpolarized beam, the background under the peak of interest typically required a correction of about 1% to the peak sum. A typical spectrum is shown in Fig. 4; this spectrum was obtained for an $^{16}\text{O}(d,\alpha)^{14}\text{N}$ reaction energy of 7.43 MeV, which corresponds to 7.0 MeV in the $^{208}\text{Pb}(d,p)^{209}\text{Pb}$ reaction.

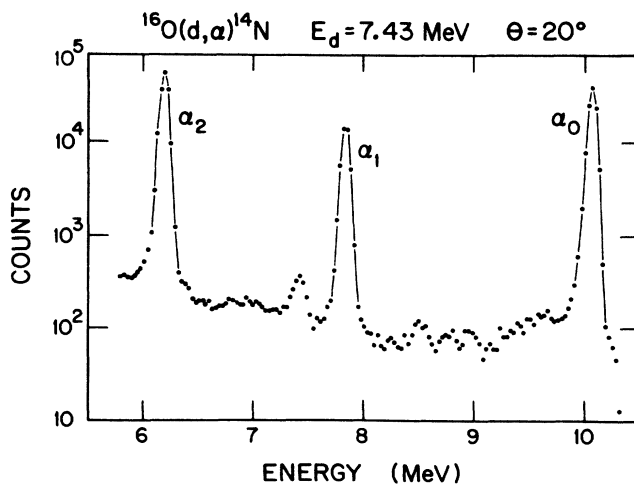


FIG. 4. Pulse-height spectrum for deuterons incident on natural oxygen at 7.43 MeV and at a laboratory angle of 20° , obtained with unpolarized beam. The three principle peaks visible correspond to alpha particles leaving the residual nucleus in the ground state and the first two excited states. The background under the group corresponding to the first excited state was about 1% of the total number of counts in the peak for each calibration energy.

Separate absolute calibrations were carried out for the two $^{208}\text{Pb}(d,p)^{209}\text{Pb}$ energies. For the Xe case, a single absolute calibration was made at a point roughly midway between the polarimeter energies needed for the 4.5- and 5.5-MeV measurements. The calibration of the polarimeter for the Xe measurements at 4.5 and 5.5 MeV was then determined relative to this absolute calibration by the use of slowing foils.²⁶ The polarization of the beam was first determined by choosing a slowing foil and a beam energy to give deuterons with an energy equal to the energy of the absolute calibration. The foil was then removed or replaced by a thicker foil so that the energy at the polarimeter was the same as that for the xenon stripping measurements. The polarimeter T_{20} analyzing power was then calculated from the polarimeter peak sums, assuming that the t_{20} beam polarization remained constant. The cycle was repeated several times, to reduce the effect of possible slow drifts in the beam polarization.

Calculations of reaction kinematics show that (d,α) reactions on ^{14}N and ^{18}O are not resolved from the $^{16}\text{O}(d,\alpha_1)^{14}\text{N}$ group. These final states were not accounted for in the original calibration of the polarimeter,²⁴ and are a potential source of error in that calibration. To assure that the target was not contaminated with nitrogen for the present calibration, the chamber was flushed continuously with high-purity oxygen. A feedback system was used to stabilize the target pressure, and monitor detectors were used to assure that nitrogen contamination of the target was negligible. Measurements of the cross section and analyzing power in the $^{18}\text{O}(d,\alpha)^{16}\text{N}$ reaction were made to determine whether a correction to the $^{16}\text{O}(d,\alpha_1)^{14}\text{N}$ peak sum was required. At each of the present calibration energies this correction was found to be negligible compared to the statistical uncertainty in the calibration.

The $^3\text{He}(d,\alpha)$ and (d,p) analyzing powers determined by the calibration are summarized in Ref. 26. The T_{20} calibrations are accurate to 0.6–0.7 % for the ^{208}Pb measurements and 0.8–0.9 % for the ^{136}Xe measurements. No new calibration was carried out for the measurement of T_{21} .

IV. DWBA ANALYSIS

A. Background

For a number of reasons, DWBA calculations are expected to be very reliable for sub-Coulomb (d,p) reactions.^{28,29} First of all, at the incident energies chosen, the Coulomb barrier excludes the incident particle from the region near the nucleus, so that the stripping process takes place at very large nuclear separations (the contributions from tunneling through the barrier are small). At large distances, the nuclear potential has little effect on the reaction; furthermore, the scattering wave functions are nearly pure Coulomb waves, and therefore can be calculated accurately.

For the final states of interest in the ^{208}Pb reaction the Q values are close to zero. This is advantageous since the incoming and outgoing wave functions peak at nearly the same radial distance. This enhances the overlap of the

initial- and final-state wave functions in the region beyond the influence of the nuclear potential, thereby decreasing the relative contribution from the nuclear interior. The ^{136}Xe reactions have larger Q values, and therefore we might expect that the transition amplitude for these reactions will be more sensitive to the nuclear potential.

The target nuclei chosen both have closed neutron shells, and this has beneficial consequences. The absence of strongly excited low-lying collective states combined with the fact that the final states have large single-particle spectroscopic factors insures that multistep processes are insignificant in comparison to the direct one-step process, and therefore that the DWBA theory is applicable. Another consequence of the closed neutron shells is that one can find well-isolated final states for which the neutron is loosely bound to the target nucleus so that the resulting wave function falls off slowly outside the nucleus. This enhances the overlap of the bound-state wave function with the scattering states which enhances the cross section (enabling one to use lower bombarding energies) and further decreases the relative importance of contributions from the nuclear interior.

B. Details of the calculations

The DWBA calculations were carried out with a version of the computer code PTOLEMY (Ref. 23) which has been modified⁸ to include spin degrees of freedom and to permit the use of noncentral (i.e., tensor) terms in the optical potentials. The calculations are full finite range, and include corrections for the stretching (electric polarization) of the deuterons by the Coulomb field of the nucleus.

Although the DWBA calculations are not very sensitive to nuclear interactions between the target and the projectiles, it is still important to exercise some care in choosing the optical potentials. We have chosen to use the global potentials of Daehnick, Childs, and Vrcelj³⁰ for the deuterons and of Becchetti and Greenlees³¹ for the protons. In addition, for the deuterons, we include tensor potentials of the form

$$V = [V_{\text{TR}}(r) + iW_{\text{TR}}(r)]T_r, \quad (4)$$

where

$$T_r = (\mathbf{s} \cdot \hat{\mathbf{r}})^2 - \frac{2}{3}. \quad (5)$$

The tensor potential is particularly important since it has a direct effect on the (d,p) tensor analyzing powers. The existence of a tensor potential with both real and imaginary parts is predicted by the folding model, and the resulting potentials have been parametrized in a convenient form by Keaton and Armstrong.³²

There is some question, however, as to whether the folding model accurately predicts the strength of the nuclear tensor potential.^{33,34} On one hand, Knutson and Haeberli³⁵ found that sub-Coulomb elastic scattering measurements for deuterons incident on ^{208}Pb at 9.0 MeV and ^{90}Zr at 5.5 MeV agree well with the predictions of the folding model. On the other hand, Kammeraad and Knutson³⁶ have found that for 8-MeV deuterons on

^{208}Pb , the elastic scattering data are reproduced more accurately if the imaginary part of the tensor potential is set to zero. Finally, Tostevin has shown that these same 8-MeV data can be explained as an effect of coupling to the (d,p) reaction channels, which suggests that the optical potential should contain an imaginary tensor term.³⁷

The situation for ^{136}Xe appears to be similar. We have measured the T_{20} analyzing power in $^{136}\text{Xe}(d,d)^{136}\text{Xe}$ elastic scattering at 5.5 MeV. The data are shown in Fig. 5 along with predictions of the folding model. If we use the full potential of Keaton and Armstrong (KA) the predicted analyzing powers (solid curve) are considerably larger in magnitude than the measurements. Reasonable fits to the data can be obtained by omitting either the real or the imaginary part of the potential or by dividing both potentials by a factor of two (dashed curve). We find that the 8-MeV ^{208}Pb data of Ref. 36 can also be reproduced reasonably well by omitting either the real or imaginary term, or by reducing both terms by a factor of 2. Since it is unclear which of the tensor depths should be adjusted to fit the data, we have chosen to scale both the real and imaginary tensor depths by a common factor. Thus, the tensor potential we have used in the DWBA calculations is just the KA potential reduced by a factor of two. The effect that the uncertainty in the potential has on the determination of η will be discussed in Sec. IV D.

In addition to the nuclear potential we include a long-range tensor potential

$$V_{QT} = \frac{3}{2} QZe^2 r^{-3} T_r, \quad (6)$$

which arises from the interaction of the deuteron quadrupole moment with the electric-field gradient of the target

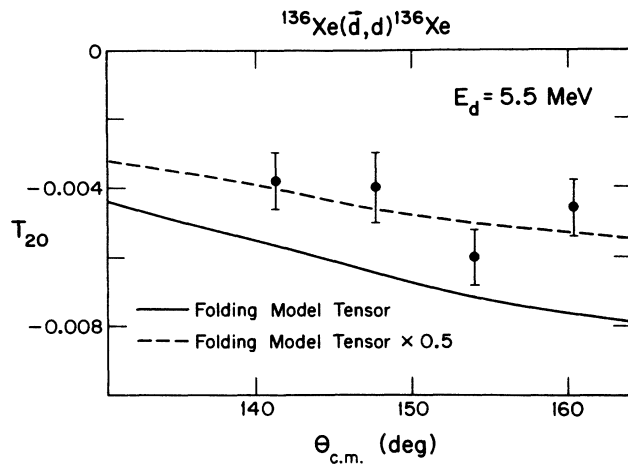


FIG. 5. Measurements of T_{20} for deuteron elastic scattering from ^{136}Xe at 5.5 MeV compared with the predictions of the folding model. The contribution of the quadrupole tensor potential to the analyzing powers has been calculated classically (Ref. 32), and has been included in both curves; the polarizability term has a smaller effect on the analyzing powers in elastic scattering, and has been neglected. The solid curve results from calculations using the KA parameters for the folding model tensor potential. The dashed curve best fits the data, and results from scaling the KA potential by a factor of 0.5. The data determine the scale factor to a statistical uncertainty of $\pm 20\%$.

nucleus. Since this potential is purely electromagnetic, the radial dependence is unambiguous, and the strength (proportional to the deuteron quadrupole moment) is well known.

There is also a long-range potential that arises from electric polarization of the deuteron in the Coulomb field of the target nucleus (see for example Ref. 38). This potential is given by the expression

$$V_P = -\frac{1}{2} Z^2 e^2 r^{-4} (\alpha + 3\tau T_r). \quad (7)$$

The polarization potential consists of a central term (proportional to α), and a tensor term (proportional to τ) which arises from the fact that the deuteron is more easily polarized when the electric field is along the spin axis. In our calculations the central term is discarded since it has a negligible effect on the analyzing powers, while for the tensor term we use $\tau = 0.0343 \text{ fm}^3$, as calculated by Lopes *et al.*³⁸

This Coulomb stretching of the deuteron also has the effect of modifying the deuteron internal wave function, so that at the point of interaction with the target the wave function differs from that of an isolated deuteron. The main effect is to introduce P -state admixtures (which for an isolated deuteron are disallowed by parity conservation) into the $n-p$ relative wave function. These admixtures correspond to virtual excitation of P states which are present in the deuteron breakup channel. Distortion of the target nucleus can be neglected, since the targets used have no low-lying collective states.³⁹

Tostevin and Johnson⁴⁰ have calculated the influence of the P -state admixtures in the deuteron wave function on the tensor analyzing powers, and have found that their contribution is small (approximately 2%), but not negligible. In Tostevin and Johnson's calculations the P -state admixture in ϕ_d is calculated at each point along the trajectory with the adiabatic approximation, and this modified deuteron wave function is used in evaluating the DWBA transition amplitude. The percentage correction is the same for each of the T_{2q} . The procedure we use is to carry out a conventional finite-range DWBA calculation using the free-deuteron wave function, and then apply the corrections as calculated by Tostevin and Johnson to the resulting analyzing powers. These corrections are listed in Ref. 26.

C. Extracting a value for η

The results of the DWBA calculations (including all corrections) are shown by the curves in Figs. 2 and 3. For these calculations we have adopted the Reid soft-core deuteron wave function, for which $\eta = 0.0263$. Since we have completely specified the optical potentials as well as the $n-p$ interaction, these calculations contain no free parameters.

To extract an empirical value of η from these measurements, we make use of the fact that the calculated analyzing powers are very nearly proportional to the value of η used in the DWBA calculations.¹⁹ Thus, the value of η which provides the best fit to the data is found by minimizing the quantity

$$\chi^2 = \sum_i \frac{\left[\left(\frac{\eta}{\eta_0} \right) C_i - M_i \right]^2}{\sigma_i^2}, \quad (8)$$

where the M_i are the measured analyzing powers, σ_i are the statistical uncertainties in the measurements, C_i are the corresponding DWBA predictions of the analyzing powers, and η_0 (0.0263) is the value of η used in the DWBA calculations.

We have extracted separate values of η from each of the ten angular distributions. The results are summarized in Table II, along with the statistical uncertainties ($\Delta\eta_S$), the minimum χ^2 per degree of freedom (χ^2/N), the corresponding confidence level, and the number of points in the angular distribution. It must be understood that the value listed for χ^2/N is based only on the uncertainties in the individual data points (which include the statistical errors plus the uncertainty in the background and contaminant subtraction). In spite of this, the average value of χ^2/N is close to one. This provides evidence that the DWBA calculations adequately reproduce the shape of the angular distributions.

Figure 6 shows a comparison of the ten individual measurements of η . The error bars shown here represent the statistical uncertainties only. It is significant that all of the values are in good agreement to within statistical errors. The consistency of the individual measurements is a strong argument for the validity of the sub-Coulomb technique for extracting η . This is particularly significant in view of the fact that the various data sets are sensitive to different experimental and theoretical problems. For example, as will be discussed below, the DWBA calculations for the 5.5-MeV ^{136}Xe data show a significant degree of sensitivity to the optical model potentials. Our estimate of the resulting systematic uncertainty in η is roughly a factor of 3 larger than the statistical error shown in Fig. 6. The fact that the results for this case (the last two data points in Fig. 6) agree well with the value extracted from the ^{208}Pb measurements, where the sensitivity to the optical-model potentials is small, offers further evidence of the reliability of the analysis.

D. Uncertainty in the calculations

The uncertainty in the DWBA calculation of the tensor analyzing powers stems primarily from uncertainty in

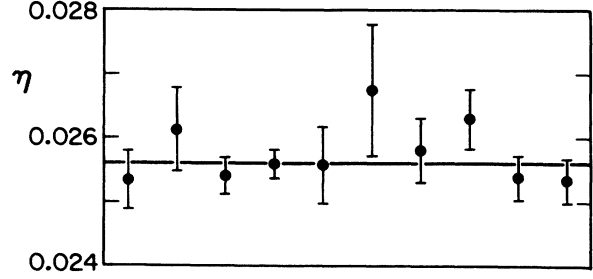


FIG. 6. Comparison of the values of η extracted from ten statistically independent angular distributions of measured tensor analyzing powers. The solid line shows a weighted average of the measurements. The value of χ^2/N calculated from the statistical uncertainties is 0.68, indicating that the results are consistent. The values are plotted in the same sequence in which they appear in Table II.

the optical potentials in the incoming and outgoing channels. To estimate the magnitude of the sensitivity of the calculations to the optical potential, we started by setting all terms of the nuclear optical potential simultaneously to zero. The effect of the nuclear potential on the calculations of T_{20} for the ^{208}Pb target at 7.0 MeV, for example, was to alter the analyzing powers by only 0.5%. Of course individual terms in the optical potential may have effects on the analyzing powers which cancel each other. In order to estimate the uncertainty in η resulting from the calculations we assign an uncertainty Δp_i to each parameter in the calculation. We then carry out DWBA calculations in which parameters are varied individually in order to determine the sensitivity of the extracted value to that parameter ($\delta\eta/\delta p_i$). The net uncertainty in the calculation, $\Delta\eta_C$, is then found by adding the contribution from the uncertainty in each of the parameters in quadrature; i.e.,

$$\Delta\eta_C = \left[\sum_i \left(\frac{\delta\eta}{\delta p_i} \Delta p_i \right)^2 \right]^{1/2}. \quad (9)$$

The main problem is to assign an uncertainty to each of the parameters of the DWBA calculations. It should be emphasized that these uncertainties are to be thought of as probable errors rather than as upper limits on the un-

TABLE II. Values obtained for η from each of the measured angular distributions of analyzing powers.

Target	T_{kq}	E_d (MeV)	E_x (MeV)	η	χ^2/N	No. pts.	C.L. (%)	$\Delta\eta_S$ (%)	$\Delta\eta_N$ (%)	$\Delta\eta_C$ (%)	Weight (%)
^{208}Pb	T_{20}	6.0	2.03	0.0253	1.8	3	17	1.8	0.7	1.1	20.3
			1.57	0.0261	0.6	3	55	2.5	0.7	1.1	10.5
		7.0	2.03	0.0254	1.4	5	23	1.1	0.6	1.5	9.7
			1.57	0.0256	0.3	4	83	0.9	0.6	1.3	44.6
			2.03	0.0256	1.3	3	27	2.4	1.0	1.3	7.7
^{136}Xe	T_{20}	4.5	1.57	0.0268	2.4	3	9	3.8	1.0	1.3	3.4
			0.00	0.0258	1.1	8	36	1.9	0.8	1.6	3.9
^{136}Xe	T_{20}	5.5	0.60	0.0263	0.7	8	67	1.8	0.8	2.0	0.0
			0.00	0.0254	1.2	8	30	1.3	0.9	3.2	0.0
			0.60	0.0253	1.7	8	10	1.3	0.9	4.5	0.0

certainty.

Choosing the uncertainties is greatly simplified by the fact that the DWBA calculations are almost totally insensitive to many of the terms in the optical potentials. The only terms for which there is an appreciable sensitivity are the deuteron tensor potentials (for both Pb and Xe) and the deuteron and proton absorptive potentials for the Xe calculation. This means that we need to take some care in assigning the uncertainties for these terms, but for the remaining terms (the real central and spin-orbit potentials and the Pb absorptive potentials) the choice of Δp_i is of little consequence. To simplify the choice of uncertainties, we have chosen to fix the radius and diffuseness parameters for all the terms in the potentials, and to assign an uncertainty to the depth which is large enough to compensate for the uncertainty in the geometry parameters.

The uncertainty in the Xe absorptive potentials was studied by fitting differential cross section measurements for proton⁴¹ and deuteron⁴² elastic scattering on ¹²⁰Sn at incident energies of 9.8 MeV and 11 MeV, respectively. We found that in the proton case a 30% variation in the absorptive depth increased the best fit χ^2 by a factor of at least 2.0. For the deuteron case we included vector analyzing power data as well as cross sections and found that a 30% change in the absorptive depth increased the best fit χ^2 by a factor of at least 1.5. These results suggest that $\pm 30\%$ could be a reasonable choice for the uncertainty in the strength of the absorptive potentials for Xe. In view of the above discussion we have adopted a $\pm 30\%$ uncertainty not only for these terms but also for the remaining central, spin orbit, and absorptive terms.

Uncertainty in the deuteron tensor potentials is a significant contribution to the uncertainty in the calculated (d,p) analyzing powers. As previously mentioned, elastic scattering of deuterons on ¹³⁶Xe at 5.5 MeV and on ²⁰⁸Pb at 8 MeV indicates that the potentials predicted by the folding model are too deep. The situation is somewhat complicated, however, since the elastic scattering data do not distinguish between the real and imaginary parts of the potential, and because the calculated analyzing powers in sub-Coulomb (d,p) reactions are sensitive to the relative strengths of the real and imaginary components of the potential.

Since either the real or imaginary folding model potential could have been adjusted to fit the elastic scattering data, we have adopted uncertainties of $\pm 50\%$ of the KA values for the real and imaginary parts of the tensor potential. This means that the real and imaginary nuclear tensor potentials are allowed to vary *independently* from zero depth to the value predicted by the folding model.

The quadrupole moment of the deuteron is known to high precision, and consequently the error introduced by the quadrupole tensor term is negligible. The electric polarizability potential does introduce a source of uncertainty in the calculations, however. Both the central polarizability (α) and the tensor polarizability (τ) have been calculated³⁸ but only α has been measured.⁴³ The central polarizability term does not influence the calculated analyzing powers, so the value of α is not critical. The comparison of its measured value with the calculations is

useful, however, since the calculated value of τ should be as reliable as the value calculated for α . Since the measured value of α agrees with the calculations within the 10% accuracy of the measurement, we have assigned an uncertainty of 10% to the value of τ calculated by Lopes.³⁸

In summary, the value of $\Delta\eta_C$ is calculated for each angular distribution by using $\Delta p = 0$ for all of the radius and diffuseness parameters in the optical potentials, $\Delta p = \pm 30\%$ for the central and spin-orbit well depths, $\Delta p = \pm 50\%$ of the KA value for the nuclear tensor potential, and $\Delta p = \pm 10\%$ for the tensor polarizability potential. The potential well used to generate the wave function of the final-state neutron has a negligible influence on the calculated analyzing powers as long as the empirical separation energy is reproduced.

The net uncertainty in the calculations is found by adding the contribution from uncertainty in each of the parameters in quadrature, as shown in Eq. (9). In addition, we have chosen to add an additional uncertainty of $\pm 1.0\%$ of the calculated analyzing powers in quadrature to this result, to account for effects not specifically investigated, such as errors related to relativistic corrections, channel coupling, etc.

Table II summarizes the uncertainties in the individual measurements of η arising from statistical uncertainty ($\Delta\eta_S$), uncertainty in the beam polarization ($\Delta\eta_N$), and uncertainty in the calculations ($\Delta\eta_C$).

V. RESULTS

In order to obtain our final result for η we need to take a weighted average of the values extracted from each of the ten angular distributions, with weighting factors chosen to minimize the uncertainty in the final result. Because the errors arise from a variety of sources, which are correlated in different ways, the problem of choosing the weighting factors is not trivial. Of course, the statistical errors of the individual measurements are completely uncorrelated. On the other hand, we assume that the uncertainty in the calculations is fully correlated among the ten measurements. This is reasonable since the same assumptions have been used to define the optical potentials in all of the calculations, so that an error present in any one calculation will be present in all. Independent calibration of the polarimeter at each energy causes the calibration errors to be uncorrelated from one energy to the next, but the calibration errors for the two final states at a given energy are correlated.

The optimum weights were determined iteratively by adjusting the weight given to each of the ten measurements one by one, with the constraint that the sum of the weights be equal to one. The weight given to each of the measurements is listed in Table II. Since the uncertainties in the calculations for the ¹³⁶Xe reactions at 5.5 MeV and for the $\frac{3}{2}^-$ final state at 4.5 MeV are so large, the uncertainty is minimized when these three measurements are given zero weight. The weighted average of the individual results and our final result for η is

$$\eta = 0.0256 \pm 0.0004 . \quad (10)$$

This result is indicated by the line in Fig. 6.

As a consistency check, it is interesting to extract a single value of η by simply fitting all of the analyzing power measurements, ignoring correlations in the uncertainties. When this is done we obtain the same value of 0.0256 for η . The agreement of the two results is meaningful since the weights given to the individual results are much different in the two cases. For example, the ^{136}Xe data are given a weight of 39%, while these data are given 4% weight in obtaining the result in Eq. (10). The consistency of the entire data set is good, with $\chi^2/N = 1.11$. For 52 degrees of freedom, this corresponds to a confidence level of 29%. Since the calculation of χ^2 neglects uncertainties associated with the calculations and the normalization, the relatively high confidence level indicates that there is little systematic dependence on the choice of target, final state, or bombarding energy in the resulting value of η , and therefore serves as evidence of the dependability of our result.

VI. DISCUSSION

A. Comparison with previous measurements

The value for η which we have obtained is smaller than most previous measurements (see Table I), and in several cases the discrepancy is sufficiently large that the error bars do not overlap. This may be misleading, however, since many of the previous results omit sources of systematic uncertainty which may be substantial.

Among the values obtained by pole extrapolation, the one bearing the smallest quoted uncertainty is that of Borbely *et al.*¹¹ While the current measurement differs from this result by 6.25% the quoted uncertainties are each only 1.5%, corresponding to a confidence level of only 0.3%. Because the uncertainty claimed by Borbely *et al.* neglects possible systematic errors in the extrapolation process, these errors may account for the difference. A careful examination of the extrapolation errors as well as other systematic errors in this result would be very useful.

There may well be some concern over the disagreement between the present result and that extracted from previous sub-Coulomb (d,p) measurements.⁸ However, in this case the statistical likelihood of obtaining the observed values of η is 9.3%, which means that the results are not totally incompatible. In fact, the reasons for the discrepancy are at least partially understood. First, the recalibration of the polarimeter changed the overall normalization of the T_{20} analyzing power by 1.2% at 7 MeV (the only energy that the two experiments have in common). Second the authors of Ref. 8 used the full folding model tensor potential (which, as discussed above, is not consistent with the elastic scattering measurements) whereas we have scaled this potential down by a factor of 2. This leads to an additional 0.6% change in the extracted value of η . In both of these cases, the effect of applying the appropriate correction to the results of Ref. 8 is to move the extracted value of η closer to the present result.

B. Comparison with theoretical values

Theoretical values obtained for η from some of the popular $n-p$ potential models are listed in Table I. In comparing the value of η obtained from any potential model with the measured value, it is important to consider the value of the pion-nucleon coupling constant used in generating the potential. It has been shown⁵ that the value obtained for η is sensitive to the strength of the pion-nucleon coupling, and consequently some of the models are out of date since they do not utilize the latest value of the coupling constant (0.0776 ± 0.0009).⁴⁴ For example, the Reid potentials use a value of 0.07574, while the Paris potential uses 0.0780.

A theoretical value for η has been obtained by Klarsfeld *et al.*⁶ by assuming that the deuteron wave function is described by the nonrelativistic Schrödinger equation, that the one-pion exchange potential dominates at distances greater than some value R_{max} , and that the complete wave function (including the interior region) must agree with the measured properties of the deuteron. The deuteron properties that are included in this analysis are the deuteron binding energy, the quadrupole moment, the effective range parameter, $\rho(-B, -B)$, and the mean-square charge radius. These constraints lead to Schwarz inequalities which place limits on the acceptable values of η . Using the value $R_{\text{max}} = 1.6$ fm, Klarsfeld *et al.* arrive at the result

$$0.0261 \leq \eta_{\text{th}} \leq 0.0275, \quad (11)$$

or alternatively $\eta_{\text{th}} = 0.0268 \pm 0.0007$. Although our experimental value for η is somewhat smaller than this result, the error bars on the two values nearly overlap and therefore the inconsistency is not of great significance.

Ericson and Rosa-Clot⁵ have used a different approach in which the asymptotic D -state wave function is assumed to be constrained by the S -state wave function and the one-pion exchange tensor potential. With the added assumption that the nucleons are point-like, it is possible to find a solution of the coupled equations for the deuteron S -state and D -state wave functions which provides a value for η . Including two-pion exchange potentials decreases the result by about 4%, which shows that η is fairly well constrained by single-pion exchange. When small corrections to the potentials are included for relativistic effects and for tensor interaction of the nucleon magnetic dipole moments, the result is

$$\eta_{\text{th}} = 0.0259 \pm 0.0003. \quad (12)$$

The quoted uncertainty in this result arises primarily from the uncertainty in the pion-nucleon coupling constant, which fixes the strength of the pion exchange potential. Although this result is in good agreement with our experimental determination of η , there has been some debate about whether the quoted error is realistic.^{6,45-47} It has been suggested that the value obtained is not truly model independent, and that the model chosen dictates the result obtained.

In calculating a value for η , Ericson and Rosa-Clot have made the assumption that the interaction between the nucleons and pions is point-like. It is interesting to

consider how the potentials and the resulting value for η are modified when the finite size of the nucleons is taken into account. The approach taken by Ericson and Rosa-Clot is to terminate the one-pion exchange (OPE) potential at some minimum distance where the nucleons lose their identity. This serves as a first approximation for the pion-nucleon form factor. The result is that the value of η decreases by an amount which depends on the cutoff radius employed. In fact, a reduction of about 1% in η from the theoretical value of 0.0259 to our result, 0.0256 implies a cutoff radius of about 0.1 fm. This is quite small compared to the rms radius of a proton (0.8 fm)⁴⁸ and implies that nucleons behave effectively as point particles. According to the results obtained in Ref. 6, a cutoff radius of 0.8 fm would give the result $\eta=0.0242$, and is completely inconsistent with measurements

Guichon and Miller⁴⁹ have improved on Ericson's calculation by recognizing that inside the cutoff radius the constituent quarks and gluons generate tensor interactions which may make up for some of the depletion of the deuteron D state caused by loss of pion exchange inside the cutoff radius. By using properly antisymmetrized wave functions within a 6-quark bag, they have been able to show that larger cutoff radii are not ruled out. That is to say, the bag model description can accommodate relatively large bag radii, yet with less impact on η than is the case with the model of Ericson and Rosa-Clot. In Guichon and Miller's calculation a cutoff radius of about 0.8 fm leads to about a 1% reduction in η compared to the result obtained with point-like nucleons.

The disagreement between the value we have obtained and that obtained by Stoks *et al.*⁷ is particularly large. The small error bar quoted with their result (0.027 12±0.0022) leads to a significant disagreement between the two results, with a confidence level of only 0.1% that both results are statistically valid. The authors of Ref. 7 have stated that the quoted error involves only statistical sources of uncertainty, and that a more complete discussion will be given in a forthcoming paper. We cannot speculate as to the possible size of these errors. It is interesting, however, that their analysis involves a model which excludes contributions of Δ and N^* components in the deuteron wave function. Nucleon-nucleon potentials which explicitly include a Δ component in the deuteron wave function favor values of η which are

slightly smaller than those obtained in traditional calculations.^{50,51} These models successfully fit the static properties of the deuteron, and lead to values for η ranging from 0.0251 to 0.0258, agreeing well with the present measurement.

These results suggest that our value of η , although somewhat smaller in magnitude than the value obtained in most previous experiments, can easily be reconciled with theoretical models of the nucleon-nucleon interaction, particularly if the internal degrees of freedom of the nucleons are taken into account.

VII. SUMMARY

The current experiment incorporates a number of significant improvements over previous sub-Coulomb (d,p) experiments including the use of lower bombarding energies (to reduce uncertainties associated with nuclear interactions), an improved polarimeter calibration, and the use of improved experimental techniques such as fast spin switching. In addition we have obtained data under diverse experimental conditions allowing, for the first time, meaningful consistency checks.

By comparing the measurements with DWBA calculations of the tensor analyzing powers, we have extracted ten statistically independent values for η . These values are consistent with each other, increasing our confidence in the result. When a weighted average of the individual results is formed, we obtain $\eta=0.0256\pm 0.0004$, where the uncertainty includes the contributions from statistics, calculations, and normalization.

In light of possible systematic errors in values of η obtained using pole-extrapolation techniques, we believe that our result is the most reliable determination currently available for η .

ACKNOWLEDGMENTS

The authors would like to thank Dai Dee Pun Casavant for her assistance in calibrating the polarimeter, and Jeff Tostevin for providing the computer code used to calculate corrections to the analyzing powers related to deuteron stretching. This work was supported in part by the National Science Foundation.

*Present address: Department of Physics, University of Alberta, Edmonton, Alberta, Canada T6G 2J1.

¹J. L. Friar, Phys. Rev. C **20**, 325 (1979).

²N. L. Rodning and L. D. Knutson, Phys. Rev. Lett. **57**, 2248 (1986).

³R. V. Reid, Ann. Phys. (N.Y.) **50**, 411 (1968).

⁴M. Lacombe, B. Loiseau, R. Vinh Mau, J. Cote, P. Pires, and R. de Tournell, Phys. Lett. **101B**, 139 (1981).

⁵T. E. O. Ericson and M. Rosa-Clot, Nucl. Phys. **A405**, 497 (1983); Ann. Rev. Nucl. Part. Sci. **35**, 271 (1985).

⁶S. Klarsfeld, J. Martorell, and D. W. L. Sprung, J. Phys. G **10**, 165 (1984).

⁷V. G. J. Stoks, P. C. van Campen, W. Spit, and J. J. de Swart,

Phys. Rev. Lett. **60**, 1932 (1988).

⁸R. P. Goddard, L. D. Knutson, and J. A. Tostevin, Phys. Lett. **118B**, 241 (1982).

⁹J. Horacek, J. Bok, V. M. Krasnopolskij, and V. I. Kukulin, Phys. Lett. B **172**, 1 (1986).

¹⁰W. Gruebler, V. Koenig, P. A. Schmelzbach, B. Jenny, and F. Sperisen, Phys. Lett. **92B**, 279 (1980).

¹¹H. E. Conzett, F. Hinterberger, P. von Rossen, F. Seiler, and E. J. Stephenson, Phys. Rev. Lett. **109B**, 262 (1982).

¹²R. D. Amado, M. P. Locher, and M. Simonius, Phys. Rev. C **17**, 403 (1978).

¹³I. Borbely, W. Gruebler, V. Koenig, P. A. Schmelzbach, and B. Jenny, Phys. Lett. **109B**, 262 (1982).

- ¹⁴J. T. Londergan, C. E. Price, and E. J. Stephenson, *Phys. Lett.* **120B**, 270 (1983).
- ¹⁵D. D. Pun Casavant, J. G. Sowinski, and L. D. Knutson, *Phys. Lett.* **154B**, 6 (1985).
- ¹⁶P. C. Colby, *Nucl. Phys.* **A370**, 77 (1981).
- ¹⁷F. D. Santos and P. C. Colby, *Phys. Lett.* **101B**, 291 (1981).
- ¹⁸K. Stephenson and W. Haeberli, *Phys. Rev. Lett.* **45**, 520 (1980).
- ¹⁹L. D. Knutson and N. L. Rodning, *J. Phys. G* **13**, L109 (1987).
- ²⁰Madison Convention, in *Polarization Phenomena in Nuclear Reactions* (University of Wisconsin Press, Madison, 1971), p. xxv.
- ²¹W. Haerberli *et al.*, *Nucl. Instrum. Methods* **196**, 319 (1982).
- ²²T. R. Wang, W. Haerberli, S. W. Wissink, and S. S. Hanna, *Phys. Rev. C* **37**, 2301 (1988).
- ²³M. H. Macfarlane and S. C. Pieper, Argonne National Laboratory Report No. ANL-76-11, 1978 (unpublished).
- ²⁴K. Stephenson and W. Haerberli, *Nucl. Instrum. Methods* **169**, 483 (1980).
- ²⁵M. Simonius, in *Polarization Nuclear Physics*, edited by D. Fick (Springer Verlag, Heidelberg, 1974), p. 38.
- ²⁶N. L. Rodning, Ph.D. thesis, University of Wisconsin, 1986, available from University Microfilms, Ann Arbor, Michigan.
- ²⁷P. L. Jolivet, *Phys. Rev. C* **8**, 1230 (1973).
- ²⁸L. D. Knutson, *Ann. Phys. (N.Y.)* **106**, 1 (1977).
- ²⁹N. Austern, *Direct Nuclear Reaction Theories*, edited by R. E. Marshak (Interscience, New York, 1970), p. 181.
- ³⁰W. W. Daehnick, J. D. Childs, and Z. Vrcelj, *Phys. Rev. C* **21**, 2253 (1980).
- ³¹F. D. Becchetti and G. W. Greenlees, *Phys. Rev.* **182**, 1190 (1969).
- ³²P. W. Keaton and D. D. Armstrong, *Phys. Rev. C* **8**, 1692 (1973).
- ³³R. P. Goddard and W. Haerberli, *Nucl. Phys.* **A316**, 116 (1979).
- ³⁴R. Frick *et al.*, *Z. Phys.* **A319**, 133 (1984).
- ³⁵L. D. Knutson and W. Haerberli, *Phys. Rev. C* **12**, 1469 (1975).
- ³⁶J. E. Kammeraad and L. D. Knutson, *Nucl. Phys.* **A435**, 502 (1985).
- ³⁷J. A. Tostevin, *Nucl. Phys.* **A466**, 349 (1987); J. A. Tostevin and R. C. Johnson, *Phys. Lett.* **124B**, 135 (1983).
- ³⁸M. H. Lopes, J. A. Tostevin, and R. C. Johnson, *Phys. Rev. C* **28**, 1779 (1983).
- ³⁹G. Baur, F. Roesel, and D. Trautman, *Nucl. Phys.* **A288**, 113 (1977).
- ⁴⁰J. A. Tostevin and R. C. Johnson, *Phys. Lett.* **85B**, 14 (1979).
- ⁴¹J. E. Durisch, R. R. Johnson, and N. M. Hintz, *Phys. Rev.* **137**, 904 (1965).
- ⁴²J. M. Lohr and W. Haerberli, *Nucl. Phys.* **A232**, 381 (1974).
- ⁴³N. L. Rodning, L. D. Knutson, W. G. Lynch, and M. B. Tsang, *Phys. Rev. Lett.* **49**, 909 (1982).
- ⁴⁴P. Kroll, in *Physics Data* (Fachinform-Zentrum, Karlsruhe, 1981), Chap. 22.1.
- ⁴⁵S. Klarsfeld, J. Martorell, and D. W. L. Sprung, *J. Phys. G* **10**, L205 (1984).
- ⁴⁶S. Klarsfeld, J. Martorell, J. A. Oteo, M. Nishimura, and D. W. L. Sprung, *Nucl. Phys.* **A456**, 373 (1986).
- ⁴⁷T. E. O. Ericson and M. Rosa-Clot, *J. Phys. G* **10**, L201 (1984).
- ⁴⁸Yu K. Akimov *et al.*, *Zh. Eksp. Teor. Fiz.* **62**, 123 (1972) [*Sov. Phys.—JETP* **35**, 651 (1972)]; *Yad. Fiz.* **29**, 649 (1979) [*Sov. J. Nucl. Phys.* **29**, 335 (1979)].
- ⁴⁹P. A. M. Guichon and G. A. Miller, *Phys. Lett.* **134B**, 15 (1984).
- ⁵⁰W. P. Sitarski, P. G. Blunden, and E. L. Lomon, *Phys. Rev. C* **36**, 2479 (1987).
- ⁵¹R. Dymarz and F. Khanna, *Nucl. Phys.* (in press).